SAND2015-0751J

Defect-reduction mechanism for improving radiative efficiency in InGaN/GaN light-emitting diodes using InGaN underlayers

Andrew. M. Armstrong,[1] Benjamin N. Bryant, Mary H. Crawford, Daniel D. Koleske, Stephen R. Lee, and Jonathan J. Wierer, Jr.

Sandia National Laboratories, Albuquerque, NM 87185 USA

The influence of a dilute $In_xGa_{1-x}N$ ($x \sim 0.03$) underlayer (UL) grown below a single $In_{0.16}Ga_{0.84}N$ quantum well (SQW), within a light-emitting diode (LED), on the radiative efficiency and deep level defect properties was studied using differential carrier lifetime (DCL) measurements and deep level optical spectroscopy (DLOS). DCL measurements found that inclusion of the UL significantly improved LED radiative efficiency. At low current densities, the non-radiative recombination rate of the LED with an UL was found to be 3.9 times lower than the LED without an UL, while the radiative recombination rates were nearly identical. This suggests that the improved radiative efficiency resulted from reduced non-radiative defect concentration within the SQW. DLOS measurement found the same type of defects in the InGaN SQWs with and without ULs. However, lighted capacitance-voltage measurements of the LEDs revealed a 3.4 times reduction in a SQW-related near-mid-gap defect state for the LED with an UL. Quantitative agreement in the reduction of both the non-radiative recombination rate (3.9X) and deep level density (3.4X) upon insertion of an UL corroborates deep level defect reduction as the mechanism for improved LED efficiency.

[1] Electronic mail: aarmstr@sandia.gov

Inclusion of a dilute In composition InGaN layer grown under an InGaN/GaN multi-quantum well (MQW) stack can improve radiative efficiency.[1–8] However, the mechanism by which a dilute InGaN underlayer (UL) improves MQW radiative efficiency remains unresolved. Previous studies have attributed improved MQW photoluminescence (PL) or electroluminescence (EL) using an InGaN UL to a number of factors: (1) shortened radiative lifetime through either reduction in the quantum-confined Stark effect[3–5] or improvement in the homogeneity of InGaN quantum wells (QWs),[7,8] (2) improved electron injection efficiency into QWs,[2,6] (3) increased non-radiative lifetime (τ_{nr}) due to defect reduction in the QWs,[1,7–10] and (4) combinations thereof. Regarding the role of InGaN ULs to reduce QW defectivity, earlier studies have used temperature-dependent PL,[1] time-resolved PL,[7,11] or threading dislocation count[8,10] to ascertain a reduced density of non-radiative defect centers in the InGaN QWs. While threading dislocation density gives an indication of general crystal quality, it does not necessarily correlate with the optical quality of QWs. Indeed, it has been suggested that threading dislocations penetrating InGaN QW are benign when decorated with so-called "V-defects."[12] Band edge PL reveals the aggregate impact of defects on QW radiative properties but does not provide direct information regarding the optical or electrical properties or concentration of the dominant non-radiative deep level defect centers. Attaining this knowledge is important to aid the physical identification of the problematic defects and to devise a rational strategy to mitigate their incorporation through optimizing MQW growth conditions.

In this work, we correlated deep level optical spectroscopy[13] (DLOS) and differential carrier lifetime (DCL) measurements[14] to quantify the impact of $In_{0.03}Ga_{0.97}N$ ULs on deep level defect incorporation and non-radiative recombination rate (G_{NR}) in a single quantum well (SQW) $In_{0.16}Ga_{0.84}N$/GaN light-emitting diode (LED). The peak radiative efficiency (η_{rad}) of the LED

with an UL was measured to be ~5 times larger than for the LED without an UL. DCL measurements revealed a concomitant 3.9 times decrease in G_{NR} with the inclusion of an $In_{0.03}Ga_{0.97}N$ UL, suggesting that the increase in η_{rad} resulted from a reduced defect density. DLOS identified a deep level defect physically located in the $In_{0.16}Ga_{0.84}N$ SQW and energetically located at 1.62 eV below the conduction band minimum (E_c). Lighted capacitance-voltage (LCV) measurements showed the density (N_t) of this deep level defect was reduced by 3.4 times with an UL. The changes in N_t and G_{NR} closely agree and strongly suggest that the improved LED efficiency when including the UL results from deep level defect reduction in the SQW.

The $In_{0.16}Ga_{0.84}N$/GaN SQW LEDs studied in this work were grown on GaN-on-sapphire templates by metal-organic vapor-phase epitaxy (MOVPE). The SQW LED structure for sample 23A has an *n*-type GaN layer grown at 1050 ºC, followed by growth of a 170 nm thick $In_{0.03}Ga_{0.97}N$:Si UL at 850 ºC. The SQW was grown next and consists of an unintentionally doped (UID) 2.5-nm-thick $In_{0.16}Ga_{0.84}N$ well grown at 770 ºC surrounded by 7.5-nm-thick Si-doped GaN quantum barriers (QBs) grown at 850 ºC. A 20 nm UID GaN spacer layer was then grown, followed by a 30-nm-thick *p*-type $Al_{0.15}Ga_{0.85}N$ electron-block layer (EBL) and a 400-nm-thick *p*-type GaN contact layer. Si doping was was ~ 1×10^{18} cm^{-3} in the QB and ~ 3×10^{18} cm^{-3} in both the $In_{0.03}GaN_{0.97}N$ UL and *n*-GaN bulk. The Mg doping was ~ 3×10^{19} cm^{-3} in all the *p*-layers. The LED structure for sample 24A was nominally identical to that of sample 23A except for the omission of the $In_{0.03}Ga_{0.97}N$ UL. The compositions and thicknesses of the III-nitride layers comprising the LED heterostructure were obtained from (0002) x-ray diffraction (XRD) $\omega/2\theta$ scans using fitted dynamical diffraction simulations (Epitaxy, Version 4.3a, PANalytical B.V.).[15] The simulations assumed that the heterostructures are coherently strained

throughout. Consistent with this assumption, previous (20-25) XRD reciprocal space maps of multiple InGaN QWs grown on similar ULs find that in-plane strain relaxation in the ULs is < $4x10^{-4}$.[16] Additionally, our thin $In_{0.16}Ga_{0.84}N$ SQWs are below the Mathews-Blakeslee critical thickness for misfit-dislocation formation.[17,18]

The epitaxial material was fabricated into two different types of LEDs to perform the various measurements. For LED used in the radiative efficiency measurements, a thin (~100 Å) Ni *p*-type contact was patterned into ~125 μm diameter circles on the *p*-GaN surface. The *n*-contact was formed by electrically shorting through the *p*-GaN layer with a probe tip adjacent to the *p*-contact. For LEDs used in the DCL, DLOS, and LCV measurements, the LEDs were fabricated on a separate piece of the wafer by patterning a Ni/Au *p*-type contact into 150 μm diameter circles, dry etching 5 μm wider circular mesas, and finally patterning a Ti/Al/Ni/Au *n*-type contact around the periphery of the mesa.

The η_{rad} of the LEDs was determined by first measuring the power into a well-defined collection angle versus current. The thin Ni behaves as an anti-reflection coating as well as a *p*-type contact. It creates a simple cavity and, with knowledge of the internal emission patterns of the SQW, allows for determination of the extraction efficiency (η_{ext}).[19] The radiative efficiency is given by:

$$\eta_{rad} = \eta_{eqe}/\eta_{inj} \cdot \eta_{ext}, \quad (1)$$

where η_{eqe} is the external quantum efficiency and η_{inj} is the injection efficiency. The η_{eqe} is measured, so the only remaining unknown quantity in Eq. 1 is η_{inj}. A value of $\eta_{inj} \sim 0.95$ was used based on previous reports.[20] It is possible the injection efficiency for these LEDs may be lower, but η_{inj} is not a contributing factor when determining the difference in the non-radiative

recombination rate. Given the uncertainty of η_{inj} we plot our radiative efficiency as an estimate ($\eta_{rad,est}$).

Fig. 1(a) shows $\eta_{rad,est}$ as a function of current density (J) for the LEDs with and without an UL. The $\eta_{rad,est}$ of the LED with the UL is higher than that of the LED without the UL for all currents and has a peak efficiency that is 5 times greater. Similar radiative lifetimes are expected for both LEDs because XRD of both samples showed the QWs have the samethickness and composition. Therefore, the difference in $\eta_{rad,est}$ is likely due to a difference in τ_{nr} between the samples.

To determine the differences in non-radiative and radiative processes between the two samples, DCL analysis[14] was performed following the experimental procedure and analysis in Ref 14. The LEDs were excited with 3 μs pulses with a superimposed ~75 mW AC voltage that varied in frequency from 10 – 50 MHz. Light was collected into a photomultiplier detector, and the current into the LED was measured with a current probe. The phase difference between the current and light provided the differential carrier lifetime (τ). Fig. 1(b) shows the measured τ versus J for the two samples. The sample without an UL had a shorter τ, as expected, which is consistent with its lower radiative efficiency.

Using the measured τ and $\eta_{rad,est}$ we determined the G_{NR} and radiative recombination (G_R) rates. Figure 2(a) shows the G_{NR} divided by carrier density versus carrier density (n). At low n, where G_{NR} is dominated by Shockley-Read-Hall (SRH) defect recombination, there is a ~3.9 times difference in non-radiative recombination rate. Equating both rates to An, where A is the SRH recombination coefficient, gives $A = 2.1 \times 10^7$ s^{-1} and 8.3×10^7 s^{-1} for the samples with and without an UL, respectively. Therefore, the non-radiative lifetimes, $\tau_{nr} = 1/A$ are 4.8×10^{-8} s and 1.2×10^{-8} s for the samples with and without and UL, respectively. Figure 2(b) shows that G_R/n

versus n are nearly identical for the two samples. It is also noted that the magnitude of G_R is consistent with previous reports of InGaN quantum wells of similar In composition,[14] demonstrating the accuracy of our implementation of DCL analysis. The differing G_{NR}/n and G_R/n behavior observed by DCL confirms that differences in deep level density account for the difference in $\eta_{rad,est}$ between the samples.

DLOS was employed to examine the specific role of deep level defect reduction using an UL to improve $\eta_{rad,est}$. DLOS measures the LED photocapacitance induced by monochromatic illumination with sub-band gap light. Photocapacitance results from a change in space-charge following photoemission of a carrier from a deep level defect located in the depletion region. The optical signature of the deep level, the optical cross-section (σ^0), is defined as the optical emission rate at a given photon energy ($h\nu$) normalized to the incident photon flux (ϕ), which can be thought of physically as the optical absorbance of the deep level per unit defect. Spectral variation of σ^0 is measured from the time derivative of the photocapacitance transient at the onset of illumination divided by ϕ. DLOS measurements of the LEDs were performed at 297 K using a Xe arc lamp source filtered through a ¼ meter monochromator with mode-sorting filters at a resolution of 0.025 eV. Details of DLOS have been described previously in the literature.[13]

Electrical bias conditions for DLOS were chosen to maximize sensitivity to the InGaN SQW.[21] As a photocapacitance technique, DLOS was only sensitive to regions of the LED that lay within the depletion region. A 0.6 V electrical bias was used for DLOS so that the depletion region terminated just below the InGaN SQW as verified by capacitance-voltage (CV) measurements (not shown). Thus, DLOS was only sensitive to deep level defects located in the InGaN SQW, the GaN:Si QB, or the UID GaN spacer. The heavily p-doped EBL is almost entirely excluded from the depletion region (and hence the DLOS spectra) due to the highly

asymmetric doping between the *p*-type and *n*-type regions. A 2 V electrical fill pulse was applied after each photocapacitance transient to re-populate the deep levels in the SQW region, followed by a 30 s relaxation time to allow thermal emission from defect states to saturate.

Figure 3 shows the resulting DLOS spectra for the LEDs. The DLOS spectra of both LEDs are nearly identical and are very similar to a previous DLOS study of MQW LEDs with similar indium content in the QWs and without an UL.[21] These observations demonstrate that the inclusion of an UL does not influence the type of deep level defects incorporated in the active region of the LED. The DLOS features between 1.60 – 2.10 eV and 2.60 – 2.90 eV are of primary interest in the present study. Previous depth-resolved[21] and indium composition-dependent[22] DLOS studies of InGaN/GaN LEDs showed that these deep level absorption bands are associated with defects located in the InGaN QWs. The location of the associated defects in the InGaN SQW makes them most likely to impact τ_{nr}. Conversely, the deep level spectrum between 2.10 – 2.60 eV was previously shown to be associated with GaN layers that are less likely to influence the QW radiative recombination process.[21] The DLOS features seen for photon energies greater than the InGaN SQW band edge ~ 2.90 eV are necessarily related to the GaN QB and/or GaN spacer layers as well.

Focusing now on the InGaN SQW-related deep level spectra between 1.60 – 2.10 eV and 2.60 – 2.90 eV, these DLOS spectra were analyzed using the model of Pässler[23] for phonon-assisted defect absorption. Non-linear least-squares fits of the model for σ^o were used to determine the optical ionization energy (E_o) and the Franck-Condon energy (d_{FC}) of the defect levels. Uncertainties for E_o and d_{FC} determined from fitting to the model of Pässler are less than 0.05 eV. All changes in photocapacitance (ΔC) were positive, indicating majority carrier (electron) photoemission, thus E_o values are referenced to E_c. The fitted E_o and d_{FC} values are

indicated in Fig. 3. Photoemission occurred for $hv < E_o$ for the E_c – 1.62 eV deep level due to phonon-assisted optical absorption operative for defect centers with strong lattice coupling.[23] The E_c – 2.64 eV deep level spectrum was sharp with no evidence of phonon broadening (d_{FC} = 0 eV), consistent with an effective mass-like state. The E_c – 1.62 eV deep level appears to be the same as a previously reported InGaN-related deep level energetically located near the middle of the InGaN SQW band gap,[21,24] while the E_c – 2.64 eV deep level is energetically located near the InGaN valence band maximum.

The E_c – 1.62 eV deep level is anticipated to be the most important deep level defect in terms of non-radiative recombination, given its energetic position near the middle of the InGaN SQW band gap. Lighted capacitance-voltage[25,26] was then used to quantify [E_c – 1.62 eV] (brackets denote defect density) for the LEDs with and without an UL. LCV determines N_t by measuring the excess applied voltage (ΔV) required to maintain a constant capacitance, i.e constant depletion depth (x_d), due to the additional space-charge in the depletion region after emptying the InGaN SQW deep level.[25] Figure 4 shows ΔV as a function of x_d measured from the difference in a CV scan taken in the dark with all deep levels fully occupied and an LCV scan taken under 2.10 eV illumination where only the E_c – 1.62 eV deep level is depopulated. Also shown in Fig. 4 is the space-charge profile measured from CV showing the SQW position. Then [E_c – 1.62 eV] was calculated from the equation:[25]

$$\Delta V = \frac{q}{\varepsilon}\int_0^x xN_t(x)dx \tag{2}$$

where q is the elementary charge and ε is the semiconductor permittivity, and the limits of integration are the edges of the of the SQW relative to the EBL, i.e. the metallurgic junction.

The density of the E_c – 1.62 eV deep level for the LED with an UL was calculated to be 1.5×10^{15} cm^{-3} compared to 5.1×10^{15} cm^{-3} for the LED without an UL, demonstrating a 3.4 times

decrease in deep level defect incorporation in the SQW when using an UL. The close agreement between the 3.4 times reduction in [E_c – 1.62 eV] and the 3.9 times increase in τ_{nr} for the LED without an UL is strong corroboration that this QW-related deep level is the dominant non-radiative recombination center in these LEDs and that the incorporation of this deep level can be greatly suppressed with the inclusion of an UL. The thermal capture cross-section of free carriers, σ_{th}, can be calculated for the E_c – 1.62 eV deep level using the usual expression $\tau_{nr} = (v_{th}\sigma_{th}N_t)^{-1}$, where v_{th} is the thermal velocity of free electrons. Taking $v_{th} = 3 \times 10^7$ cm/s along with the experimental values of τ_{nr} extracted from differential carrier lifetime analysis and N_t determined from LCV, calculations yield $\sigma_{th} = 5 \times 10^{-16}$ cm^2. This value is physically reasonable, and its derivation from direct experimental measurements of LED defect and optical properties makes it a useful datum for blue-emitting InGaN/GaN LED device simulations.

The mechanism for UL-mediated defect control is likely sequestration of point defects from the optically active SQW region, as suggested previously.[1,9] Growth is often interrupted to accommodate a drastic change in MOCVD growth conditions when transitioning from higher temperature GaN growth to lower temperature SQW and QB growth. This growth interruption has been suggested to cause excess impurity incorporation at the growth surface, which can then be incorporated in subsequently grown QWs.[1,9] Inclusion of an InGaN UL immediately after high-temperature GaN growth is interrupted may stabilize growth conditions and act as a buffer between the defective region and the optically active region in the LED. In addition to providing spatial separation between the growth-interrupt interface and the QWs, introduction of In in the growth environment when growing an UL also plays an important role in defect mitigation. Use of low temperature GaN buffer layers in lieu of InGaN ULs were found not to improve MQW PL,[1] indicating the importance of In atoms for defect suppression.[11] A depth-resolved study of

deep level defect incorporation in MQW regions of $In_{0.13}Ga_{0.87}N$/GaN LEDs without ULs also found that the InGaN QWs themselves can act to reduce the E_c – 1.62 eV defect incorporation as the MQW growth proceeds,[21] similar to the effect of a dilute InGaN UL observed in this study. Thus, it is speculated that the arrival of In atoms on the growth surface might help to bury defects and impurities that could otherwise segregate at the post-interrupt growth surface and contaminate the subsequently grown QW.

In summary, the influence of introducing an InGaN UL below the active region of a SQW $In_{0.16}Ga_{0.84}N$/GaN LED on the LED radiative and deep level defect properties was studied using DCL and DLOS measurements. It was observed that the LED with an UL had >5 times greater η_{rad}. The non-radiative lifetime of the LED with an UL was found to be 3.9 times longer DCL analysis, suggesting that improved η_{rad} resulted from reduced non-radiative deep level defect incorporation. DLOS investigation of the LEDs found the same type of defects in the InGaN QWs with and without ULs. However, LCV measurement of the SQW deep level density revealed a 3.4 times reduction in a near-mid-gap defect state at E_c – 1.62 eV for the LED with an UL. The close agreement in the magnitude of changes in τ_{NR} and [E_c – 1.62 eV] strongly suggests that the corresponding $In_{0.16}Ga_{0.84}N$ defect is the primary non-radiative center in these LEDs. A value of $\sigma_{th} = 5 \times 10^{-16}$ cm^2 was determined for defect-related non-radiative recombination.

This work was supported by the U.S. Department of Energy, Office of Science, Office of Basic Energy Sciences through the Energy Frontier Research Center for Solid-State Lighting Science and the Electronic Materials program. Sandia National Laboratories is a multi-program laboratory managed and operated by Sandia Corporation, a wholly owned subsidiary of

Lockheed Martin Corporation, for the United States Department of Energy's National Nuclear Security Administration under contract DE-AC04-94AL85000.

REFERENCES

[1] T. Akasaka, H. Gotoh, T. Saito, and T. Makimoto, Appl. Phys. Lett. **85**, 3089 (2004).

[2] M.J. Davies, F.C.-P. Massabuau, P. Dawson, R.A. Oliver, M.J. Kappers, and C.J. Humphreys, Phys. Status Solidi C **11**, 710 (2014).

[3] M.J. Davies, P. Dawson, F.C.-P. Massabuau, R.A. Oliver, M.J. Kappers, and C.J. Humphreys, Appl. Phys. Lett. **105**, 092106 (2014).

[4] T. Li, Q.Y. Wei, A.M. Fischer, J.Y. Huang, Y.U. Huang, F.A. Ponce, J.P. Liu, Z. Lochner, J.-H. Ryou, and R.D. Dupuis, Appl. Phys. Lett. **102**, 041115 (2013).

[5] N. Nanhui, W. Huaibing, L. Jianping, L. Naixin, X. Yanhui, H. Jun, D. Jun, and S. Guangdi, Solid-State Electron. **51**, 860 (2007).

[6] N. Otsuji, K. Fujiwara, and J.K. Sheu, J. Appl. Phys. **100**, 113105 (2006).

[7] J.K. Son, S.N. Lee, T. Sakong, H.S. Paek, O. Nam, Y. Park, J.S. Hwang, J.Y. Kim, and Y.H. Cho, J. Cryst. Growth **287**, 558 (2006).

[8] P.T. Törmä, O. Svensk, M. Ali, S. Suihkonen, M. Sopanen, M.A. Odnoblyudov, and V.E. Bougrov, J. Cryst. Growth **310**, 5162 (2008).

[9] T. Akasaka, H. Gotoh, Y. Kobayashi, H. Nakano, and T. Makimoto, Appl. Phys. Lett. **89**, 101110 (2006).

[10] N. Nanhui, W. Huaibing, L. Jianping, L. Naixin, X. Yanhui, H. Jun, D. Jun, and S. Guangdi, J. Cryst. Growth **286**, 209 (2006).

[11] H. Kumano, K. Hoshi, S. Tanaka, I. Suemune, X.-Q. Shen, P. Riblet, P. Ramvall, and Y. Aoyagi, Appl. Phys. Lett. **75**, 2879 (1999).

[12] A. Hangleiter, F. Hitzel, C. Netzel, D. Fuhrmann, U. Rossow, G. Ade, and P. Hinze, Phys. Rev. Lett. **95**, 127402 (2005).

[13] A. Chantre, G. Vincent, and D. Bois, Phys. Rev. B **23**, 5335 (1981).

[14] A. David and M.J. Grundmann, Appl. Phys. Lett. **96**, 103504 (2010).

[15] M.E. Vickers, M.J. Kappers, T.M. Smeeton, E.J. Thrush, J.S. Barnard, and C.J. Humphreys, J. Appl. Phys. **94**, 1565 (2003).

[16] S.R. Lee, D.D. Koleske, M.H. Crawford, and J.J. Wierer Jr., J. Cryst. Growth **355**, 63 (2012).

[17] D. Holec, P.M.F.J. Costa, M.J. Kappers, and C.J. Humphreys, J. Cryst. Growth **303**, 314 (2007).

[18] J.W. Matthews and A.E. Blakeslee, J. Cryst. Growth **27**, 118 (1974).

[19] Y.C. Shen, J.J. Wierer, M.R. Krames, M.J. Ludowise, M.S. Misra, F. Ahmed, A.Y. Kim, G.O. Mueller, J.C. Bhat, S.A. Stockman, and P.S. Martin, Appl. Phys. Lett. **82**, 2221 (2003).

[20] G. Chen, M. Craven, A. Kim, A. Munkholm, S. Watanabe, M. Camras, W. Götz, and F. Steranka, Phys. Status Solidi A **205**, 1086 (2008).

[21] A. Armstrong, T.A. Henry, D.D. Koleske, M.H. Crawford, and S.R. Lee, Opt. Express **20**, A812 (2012).

[22] A.M. Armstrong, M.H. Crawford, and D.D. Koleske, Appl. Phys. Express **7**, 032101 (2014).

[23] R. Pässler, J. Appl. Phys. **96**, 715 (2004).

[24] A. Armstrong, T.A. Henry, D.D. Koleske, M.H. Crawford, K.R. Westlake, and S.R. Lee, Appl. Phys. Lett. **101**, 162102 (2012).

[25] S.D. Brotherton, Solid-State Electron. **19**, 341 (1976).

[26] A. Armstrong, A.R. Arehart, and S.A. Ringel, J. Appl. Phys. **97**, 083529 (2005).

FIGURE 1

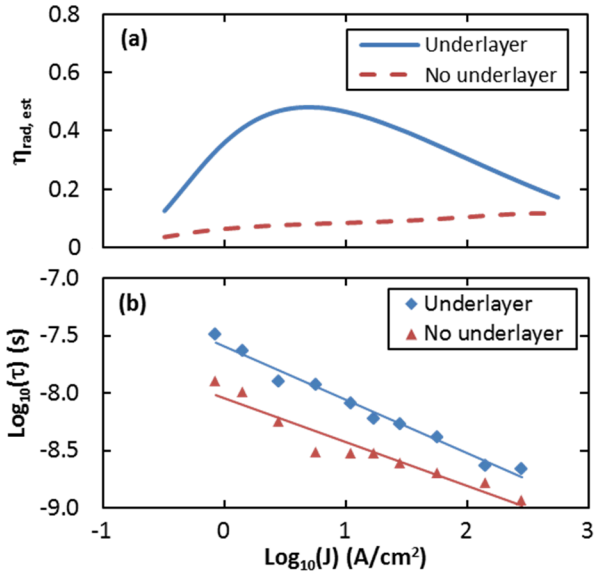

Fig. 1. Plots of (a) estimated radiative efficiency ($\eta_{rad,est}$) and (b) differential carrier lifetime (τ) versus current density (J) for the LEDs with and without an underlayer. The LED with the underlayer has higher $\eta_{rad,est}$ and longer lifetime.

FIGURE 2

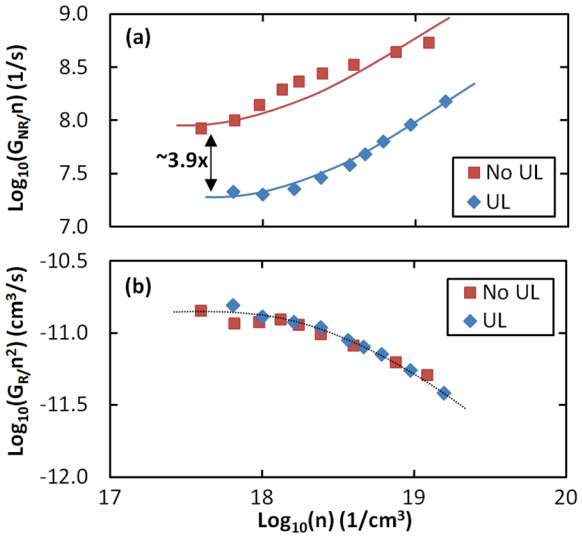

Fig. 2. Plots of (a) non-radiative recombination rate divided by carrier density (G_{NR}/n), and (b) radiative recombination rate divided by carrier density (G_R/n), versus n for LEDs with and without an underlayer. At low n, where Shockley-Read-Hall defect recombination dominates, there is a ~3.9 times difference in non-radiative recombination rate. The radiative recombination rates are nearly

FIGURE 3

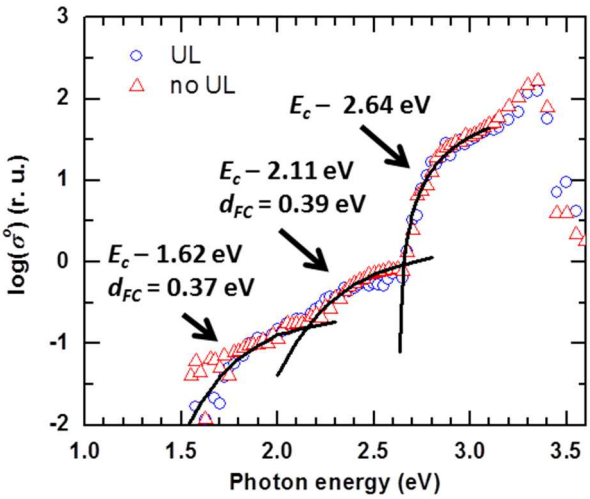

Fig. 3. DLOS spectra from the LEDs with and without an UL. The same defect states are observed in both LEDs. The solid black lines are fits to the analytical model of Pässler.[16] Note that the DLOS data are not indicative of the deep level density.

FIGURE 4

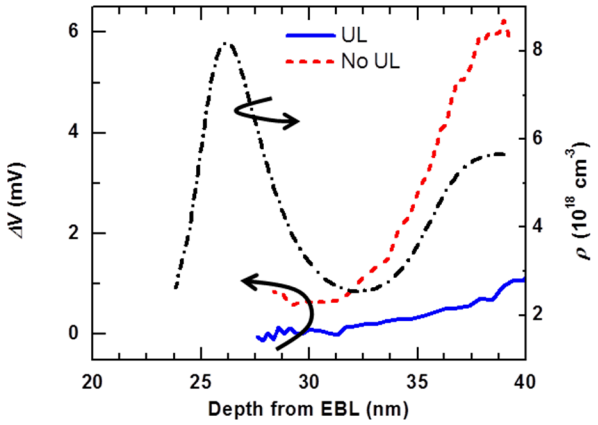

Fig. 4. Lighted capacitance-voltage data for the E_c – 1.62 eV $In_{0.16}Ga_{0.84}N$ SQW deep level for the two LEDs with and without an UL. The ΔV values are proportional to N_t, which was calculated with Eq. 2, and demonstrate reduced defect density with the inclusion of an UL. Also shown is the space-charge density profile for the LED without an UL that demarcates the position of the SQW.